

Electronic Supplementary Information (ESI) for:

Assessing the ligand properties of 1,3-dimesitylbenzimidazol-2-ylidene in ruthenium-catalyzed olefin metathesis

Yannick Borguet,^a Guillermo Zaragoza,^b Albert Demonceau,^a and Lionel Delaude*^a

^a *Laboratory of Organometallic Chemistry and Homogeneous Catalysis, Institut de Chimie (B6a), Université de Liège, Sart-Tilman par 4000 Liège, Belgium. E-mail: l.delaude@ulg.ac.be; Fax: +32 4 366 3497*

^b *Unidade de Difracción de Raios X, Universidade de Santiago de Compostela, Edificio CACTUS, Campus Vida, 15782 Santiago de Compostela, Spain*

Content:

Part 1. Detailed crystallographic analysis of [RuCl ₂ (PCy ₃)(BMes)(=CHPh)] (1d) and comparison with the structures of [RuCl ₂ (PCy ₃)(SIMes)(=CHPh)] (1a) and [RuCl ₂ (PCy ₃)(IMes)(=CHPh)] (1b)	S2
Part 2. Detailed crystallographic analysis of [RhCl(COD)(BMes)] (9) and comparison with the structures of [RhCl(COD)(SIMes)] (9a) and [RhCl(COD)(IMes)] (9b)	S4
Part 3. Bibliography.....	S7

Part 1. Detailed crystallographic analysis of $[\text{RuCl}_2(\text{PCy}_3)(\text{BMes})(=\text{CHPh})]$ (**1d**) and comparison with the structures of $[\text{RuCl}_2(\text{PCy}_3)(\text{SIMes})(=\text{CHPh})]$ (**1a**) and $[\text{RuCl}_2(\text{PCy}_3)(\text{IMes})(=\text{CHPh})]$ (**1b**)

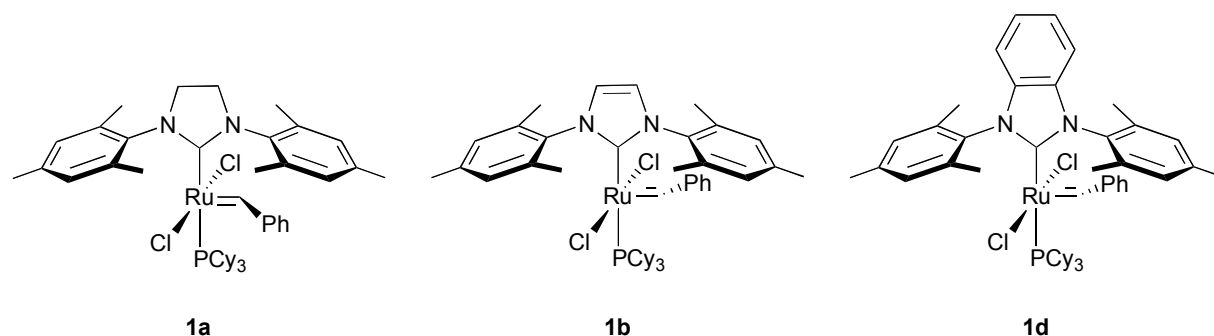


Figure S1. Structures of complexes **1a**, **1b**, and **1d**

Table S1. Main bond distances and angles for complexes **1a**, **1b**, and **1d**

Complex	1a ^a	1b ^b	1d
Bond lengths (Å)			
C1–Ru1	2.0847(19)	2.069(11)	2.060(6)
Cl1–Ru1	2.3912(5)	2.393(3)	2.3781(16)
Cl2–Ru1	2.3988(5)	2.383(3)	2.3920(16)
P1–Ru1	2.4245(5)	2.419(3)	2.4252(16)
C26–Ru1	1.835(2)	1.841(11)	1.835(6)
C1–N1	1.348(2)	1.366(12)	1.385(7)
C1–N2	1.347(2)	1.354(13)	1.376(7)
N1–C2	1.482(3)	1.428(11)	1.394(6)
N2–C7	1.476(2)	1.378(12)	1.409(7)
N1–C8	1.432(2)	1.428(11)	1.438(7)
N2–C17	1.440(2)	1.487(12)	1.453(7)
C26–C27	1.470(3)	1.40(2)	1.453(8)
Bond angles (deg)			
Cl1–Ru1–Cl2	167.707(18)	168.62(12)	168.35(6)
P–Ru1–Cx	95.89(6)	97.1(4)	97.23(18)
Cl1–Ru1–C22	103.15(7)	104.3(5)	102.6(2)
Cl2–Ru1–C22	89.14(7)	87.1(4)	89.0(2)
C1–Ru1–C22	100.24(8)	99.2(5)	97.8(2)
C1–Ru1–Cl1	83.26(5)	90.4(3)	91.24(16)
C1–Ru1–Cl2	94.55(5)	86.9(3)	86.98(16)
C1–Ru1–P1	163.73(6)	163.2(3)	163.98(17)
Cl1–Ru1–P1	91.063(18)	89.86(9)	90.83(5)
Cl2–Ru1–P1	87.753(18)	89.51(10)	87.79(5)
N1–C1–N2	107.27(16)	101.0(8)	103.7(5)
C1–N1–C8	128.39(16)	118.6(8)	127.8(5)
C1–N2–C17	127.74(16)	124.4(8)	126.8(5)

^a Data from reference 1. ^b Data from reference 2.

No significant deviations were observed between the structural data acquired for the new complex **1d** and those reported previously for the analogous second-generation ruthenium–benzylidene catalysts **1a**¹ and **1b**² (Table S1). Analysis of the short π – π ring interactions in the molecular structure of complex **1d** revealed the existence of intramolecular interactions between the aromatic ring of the benzylidene moiety and one of the mesityl substituents (Figure S2). Comparison with similar interactions in complexes **1a** and **1b** showed that they decreased in the order **1a** > **1d** > **1b** (Table S2). Thus, the BMes ligand was intermediate between IMes and SIMes in terms of coplanarity and distance relative to the benzylidene unit.

In all three complexes, the ruthenium atom lay *above* the plane defined by the N1–C1–N2 carbene unit when the phosphorus atom was placed upwards as a reference, while the *ipso*-carbon atoms of the two mesityl groups were located *behind* the same plane (Figure S3 and Table S3). The phenyl ring of the benzylidene moiety, on the other hand, was alternatively pointing toward one side or the other of the reference plane (see Figure S1 for the relative orientations).

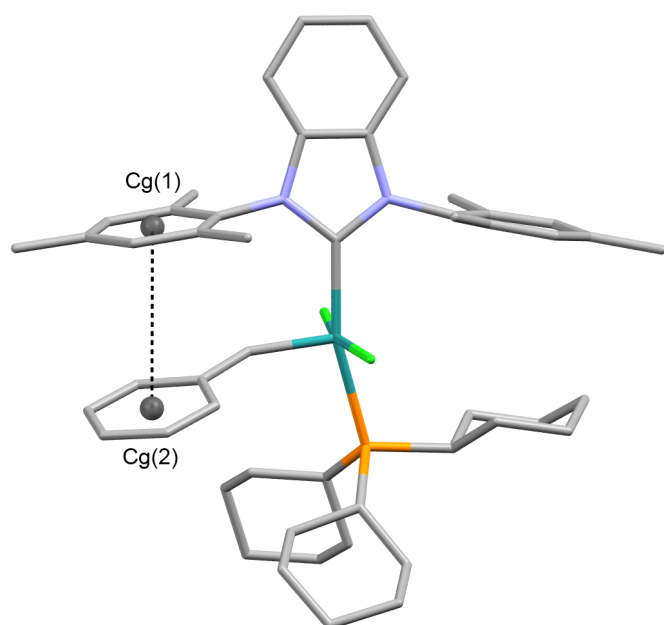


Figure S2. Short π – π ring interactions in the molecular structure of complex **1d**

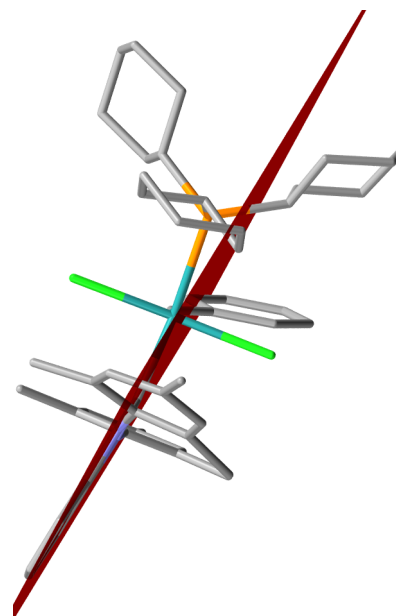


Figure S3. Deviations to planarity in complex **1d**

Table S2.

Complex	NHC	Cg(1)–Cg(2) (Å)	α (deg)	β (deg)	γ (deg)	Cg(1)_Perp (deg)	Cg(2)_Perp (deg)
1a	SIMes	3.7730	8.389	26.02	34.37	3.1142	–3.3905
1d	BMes	3.8180	12.3	24.33	36.61	–3.065	3.480
1b	IMes	3.9046	14.525	20.00	34.52	–3.2172	–3.6691

Table S3.

Complex	NHC	Ru1–P11 (Å)	C8–P11 (Å)	C17–P11 (Å)
1a	SIMes	0.276	–0.178	–0.252
1d	BMes	0.243	–0.078	–0.166
1b	IMes	0.183	–0.035	–0.187

Part 2. Detailed crystallographic analysis of [RhCl(COD)(BMes)] (**9**) and comparison with the structures of [RhCl(COD)(SIMes)] (**9a**) and [RhCl(COD)(IMes)] (**9b**)

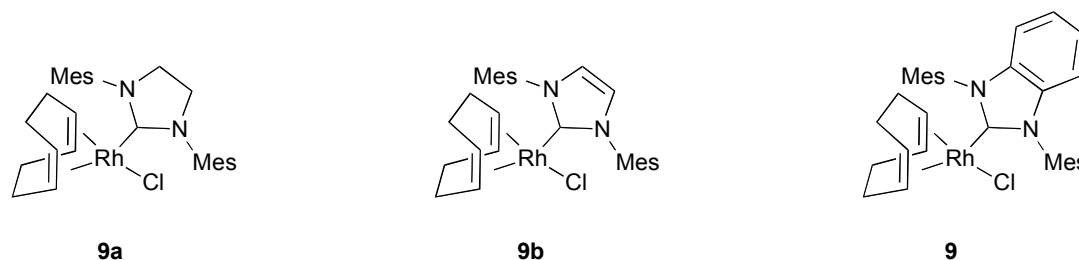


Figure S4. Structures of complexes **9a**, **9b**, and **9**

Table S4. Main bond distances and angles for complexes **9a**, **9b**, and **9**

Complex	9a ^a	9b ^b	9
Bond lengths (Å)			
C1–Rh	2.0513(14)	2.0494(16)	2.029(3)
Cl1–Rh	2.3665(3)	2.3773(4)	2.3556(9)
C22–Rh	2.1316(13)	2.1190(17)	2.096(3)
C23–Rh	2.1150(14)	2.0941(17)	2.118(3)
C26–Rh	2.2153(17)	2.2241(18)	2.180(4)
C27–Rh	2.1664(17)	2.1701(17)	2.197(3)
C1–N1	1.3455(19)	1.363(2)	1.370(4)
C1–N2	1.3557(19)	1.364(2)	1.373(4)
N1–C2	1.476(2)	1.394(2)	1.390(4))
C2–C3	1.507(3)	1.344(3)	1.385(4)
N2–C3	1.485(2)	1.391(2)	1.398(4)
N1–C4	1.439(2)	1.445(2)	1.448(4)
N2–C13	1.425(2)	1.444(2)	1.443(4)
C22–C23	1.406(2)	1.408(3)	1.383(5)
C23–C24	1.494(2)	1.512(3)	1.585(8)
C24–C25	1.517(4)	1.532(3)	1.436(7)
C25–C26	1.522(3)	1.511(3)	1.501(5)
C26–C27	1.371(4)	1.383(3)	1.370(4)
C27–C28	1.515(3)	1.515(3)	1.507(4)
C28–C29	1.533(3)	1.532(3)	1.522(8)
C29–C22	1.512(2)	1.527(3)	1.527(7)
Bond angles (deg)			
C1–Rh–C22	92.43(6)	90.80(6)	95.75(12)
C1–Rh–C23	94.49(6)	93.77(7)	96.25(13)
C1–Rh–C26	169.31(9)	171.65(7)	159.34(12)
C1–Rh–C27	154.24(9)	151.46(7)	163.58(12)
C1–Rh–Cl	91.86(4)	92.90(5)	87.52(8)
Cl1–Rh–C22	164.60(4)	167.49(5)	154.92(9)
Cl1–Rh–C23	155.30(4)	152.19(5)	165.93(9)
Cl1–Rh–C26	89.02(5)	88.84(5)	90.50(9)
Cl1–Rh–C27	87.77(5)	88.79(6)	88.19(9)
N1–C1–N2	107.29(12)	103.50(14)	104.1(2)
C1–N1–C4	127.62(13)	123.24(14)	127.4(2)
C1–N2–C13	127.06(12)	125.02(14)	127.3(2)

^a Data from reference 3. ^b Data from reference 4.

As expected, a square-planar arrangement of the ligands around the metal center was observed in complex **9**, with the NCN plane of the carbene approximately perpendicular to the coordination plane of rhodium. Altogether, the various bond lengths and angles were in line with those reported previously for [RhCl(COD)(SIMes)] (**9a**)³ and [RhCl(COD)(IMes)] (**9b**)⁴ (Table S4). The cyclooctadiene ring presented a little disorder, with two different orientations in *ca.* 65/35 ratio for the C–C single bonds linked to the C=C double bond *trans* to the halogen (C24 and C27 or C24B and C27B, see Figure S5).

Interatomic bond distances corresponding to the olefinic carbon atoms *trans* to the carbene center (Rh–C26 and Rh–C27) were slightly longer than those facing the chloro ligand (Rh–C22 and Rh–C23) (Table S4). Moreover, the C=C distances of the COD double bond *trans* to the carbene ligands (C26–C27) were shorter than those *trans* to the chloro ligand (C22–C23) in the [RhCl(COD)(NHC)] complexes under examination. These observations indicate that the three mesityl-based NHCs exerted a greater *trans* influence than the halogen. Based on this criteria, it was not possible, however, to distinguish BMes from SIMes or IMes, as the three ligands led to similar Rh–C_{COD} average distances. Variations of the average C_{carbene}–N bond lengths were slightly more pronounced among complexes **9a**, **9b**, and **9** as they increased from 1.350(3) Å with SIMes to 1.363(3) Å with IMes and 1.371(5) Å with BMes. The N–C_{carbene}–N ring angle was even more affected by the nature of the heterocycle as it decreased from 107.29(12)° for SIMes to 104.1(2)° for BMes and 103.50(14)° for IMes. These results fit nicely with those reported by Nonnenmacher *et al.* who observed a good correlation between the carbene angle and its ¹³C NMR chemical shift.⁵ Increase of the C_{carbene}–N bond distances, and decrease of the N–C_{carbene}–N ring angles when switching from “saturated” to “unsaturated” carbene backbone are well documented in the literature.⁶ They have been attributed to a decreased π -electron delocalization in the five-membered ring⁷ and an increased p-character of the carbenoid carbon.⁸

The determination of the distance between the chloro ligand and the centroid of the mesityl rings showed that the halogen atom was slightly oriented toward the C4 → C9 ring (Cg(1)) in complex **9b** featuring the IMes ligand (Figure S6 and Table S5). This effect was more pronounced in complex **9a** sporting the SIMes ligand, whereas in complex **9** the Cl atom was slightly shifted towards the C13 → C18 ring (Cg(2)).

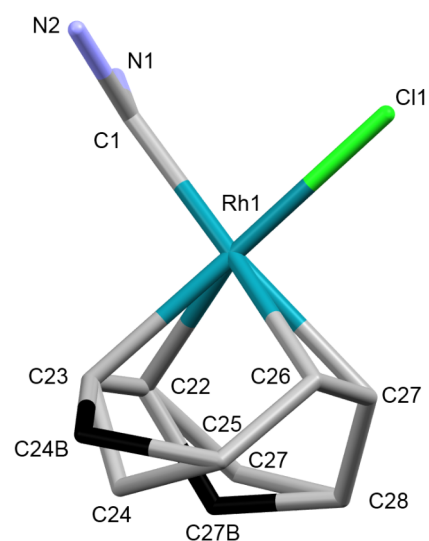


Figure S5. Disorder of the 1,5-cyclooctadiene ligand in complex **9**

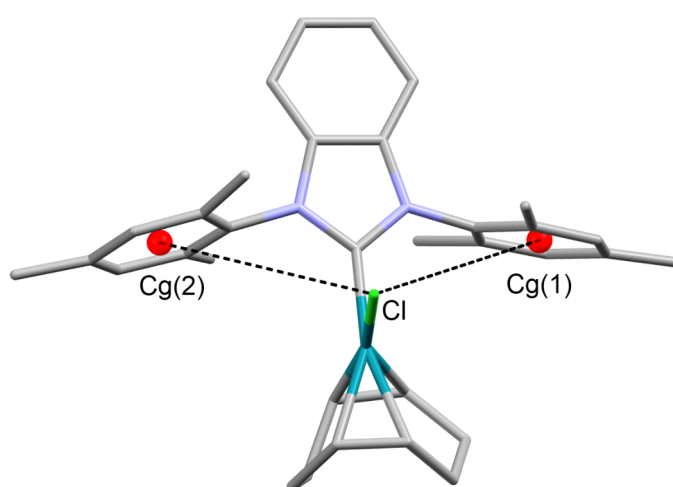


Figure S6. Orientation of the chloro ligand relative to the mesityl rings in complex **9**

Table S5.

Complex	NHC	Cl–Cg(1) (C4 → C9) (Å)	Cl–Cg(2) (C13 → C18) (Å)
9a	SIMes	3.719	5.745
9b	IMes	4.902	5.177
9	BMes	5.553	4.759

In compound **9b**, the rhodium atom lay almost exactly in the plane defined by the N1–C1–N2 carbene unit, whereas in the two other complexes under examination, the metal center and the nitrogen heterocycle were not coplanar. With the chloro substituent placed upwards as a reference, the metal was oriented *above* the BMes ligand in complex **9**, but *below* the SIMes ligand in complex **9a** (see Figure S7 and the Rh1–P11 distance in Table S6). It is also noteworthy that the *ipso* carbon atoms of the mesityl groups were located *behind* the reference plane with the IMes and BMes ligands, and *ahead* when SIMes was coordinated to the metal center (see the C4–P11 distance in Table S6). Small albeit significant deviations from planarity were also observed in ruthenium complexes of type 1 (*cf.* Figure S3 and Table S3). It should be pointed out that the % V_{Bur} parameter proposed by Cavallo and Nolan does not take into account these deviations, as the putative metal center is placed on a line located within the N1–C1–N2 plane (Figure S8).⁹ Thus, a further refinement of this model might be considered to take these experimental variations into account.

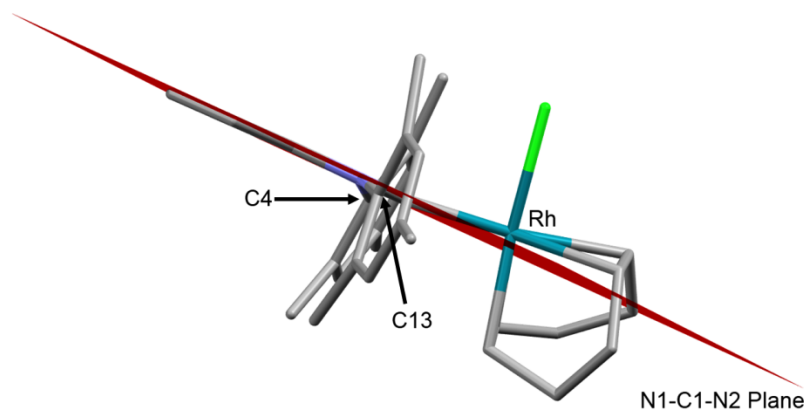


Figure S7. Deviation to planarity in complex **9**

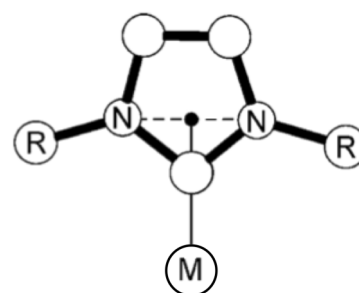


Figure S8. Geometrical building of the putative metal center for the determination of % V_{Bur}

Table S6.

Complex	NHC	Rh1–P11 (Å)	C4–P11 (Å)	C13–P11 (Å)
9a	SIMes	–0.154	0.106	0.346
9b	IMes	0.006	–0.102	–0.141
9	BMes	0.259	–0.207	–0.148

Part 3. Bibliography

1. J. A. Love, M. S. Sanford, M. W. Day and R. H. Grubbs, *J. Am. Chem. Soc.*, 2003, **125**, 10103–10109.
2. J. Huang, E. D. Stevens, S. P. Nolan and J. L. Petersen, *J. Am. Chem. Soc.*, 1999, **121**, 2674–2678.
3. A. P. Blum, T. Ritter and R. H. Grubbs, *Organometallics*, 2007, **26**, 2122–2124.
4. P. A. Evans, E. W. Baum, A. N. Fazal and M. Pink, *Chem. Commun.*, 2005, 63–65.
5. M. Nonnenmacher, D. Kunz, F. Rominger and T. Oeser, *Chem. Commun.*, 2006, 1378–1380.
6. F. E. Hahn and M. C. Jahnke, *Angew. Chem., Int. Ed.*, 2008, **47**, 3122–3172.
7. W. A. Herrmann and C. Köcher, *Angew. Chem., Int. Ed.*, 1997, **36**, 2162–2187.
8. A. J. Arduengo, III, *Acc. Chem. Res.*, 1999, **32**, 913–921.
9. A. Poater, B. Cosenza, A. Correa, S. Giudice, F. Ragone, V. Scarano and L. Cavallo, *Eur. J. Inorg. Chem.*, 2009, 1759–1766.